CHAPTER 4

GEOCHEMISTRY

4.1 SAMPLE PREPARATION

The twenty-seven carefully selected mafic volcanic rocks and hypabyssal rocks were prepared for whole-rock chemical analysis by splitting into conveniently sized fragments, and then crushing to small chips (approximately 5 mm across), using a Rocklabs Hydraulic Splitter/Crusher. The chips were cautiously chosen to avoid those containing vesicles, amygdale minerals, veinlets, xenoliths and weathering surfaces. The compressed air was used to remove dusty materials from the selected chips. Approximately 50-80 g of the cleaned chips was pulverized for a few minutes by a Rocklabs Tungsten-Carbide Ring Mill. The sample preparation was done at the Department of Geological Sciences, Faculty of Science, Chiang Mai University.

4.2 ANALYTICAL TECHNIQUES

Chemical analyses of major oxides (SiO_2, TiO_2, Al_2O_3, total iron as Fe_2O_3, MnO, MgO, CaO, Na_2O, K_2O and P_2O_5) and a range of trace elements (Rb, Sr, Y, Zr, Nb, Ni, Cr, V, Sc, Hf, Ta and Th) were carried out, using a Philips MagixPro PW 2400 Wavelength Dispersive Sequential X-Ray Spectrometer, installed at the Department of Geological Sciences, Faculty of Science, Chiang Mai University. The major oxides were measured from fusion discs, prepared by mixing 1.0 g sample powder with 5.0 g lithium tetraborate ($Li_2B_4O_7$) and 0.1 g lithium bromide (LiBr). The trace elements were determined on pellets, made by pressing mixes of 5.0 g sample powder and 1.0 g $C_6H_8O_3N_2P$ wax at 200 kN pressure. The net (background corrected) intensities were measured, and the concentrations were calculated against the calibrations derived

from eight international standard reference rock samples (AGV-2, BIR-1, RGM-1, BCR-2, DNC-1, W-2, BHVO-2 and GSP-2). The inter-element matrix corrections were done by the SuperQ version 3.0 program. The reporting detection limits are about 0.01 wt% for major oxides, 6 ppm for Cr and V, 5 ppm for Ni and Sc, 3 ppm for Rb, 2 ppm for Sr, Y, Zr, Nb, Hf and Th, and 1 ppm for Ta. All the fusion discs and pellets were prepared by the author and analyzed by Dr. Apichet Boonsoong.

Rare-earth elements (herein REE: La, Ce, Pr, Nd, Sm, Eu, Gd, Tb, Dy, Ho, Er, Tm and Yb) were determined on five representative samples, using an Inductively Coupled Plasma Mass Spectrometer (herein ICP-MS), installed at the Department of Geology, Royal Holloway College, University of London. The preparation of solutions for ICP-MS analysis can be divided into the following steps.

Step 1: 0.5 g of powdered samples and 12 ml of HF and $HClO_4$ mixture were put into platinum crucibles. The crucibles were dried on a sand bath, and removed from the sand bath and allowed to cool. 5 ml of HCl and a little distilled water were added to the crucibles and warmed up on the sand bath for 5 minutes. Then more distilled water was added to make volume about ¾ of the crucible and warmed up for a further 15 minutes or until complete dissolution. The crucibles were, again, removed from the sand bath and allowed to cool.

Step 2: The dissolved samples were filtered into a 100 ml beaker using a number 42 ashless filter paper. The filter papers were rinsed with distilled water several times to obtain the filtrates not more than 60 ml, and folded into cleaned silver crucibles and put into a furnace. The silver crucibles were heated in the furnace at 800°C in 200°C increments for 30 minutes, and removed and allowed to cool. Six pellets of sodium hydroxide were added to each sample, and the crucibles were put into the furnace at 800°C for another 30 minutes. The crucibles were separately removed, swirled until complete solidification, and allowed to cool. The crucibles were, subsequently, half filled with distilled water and left for 30 minutes to digest fusion cakes, and then 5 ml of HCl was added. The fusion portions were added to the filtered portions, and diluted to approximately 100 ml with distilled water.

Step 3: The sample solutions were loaded, and rinsed by distilled water. When all the samples have passed through the columns, the columns were eluted by 500 ml of 1.7M HCl to remove major and trace elements from the resin. Again, the columns were eluted by 600 ml of 4M HCl, and the solutions run through the columns were subsequently evaporated on a hotplate until approximately 15 ml solutions remain. The solutions were transferred to 50 ml beakers by rinsing with distilled water and evaporated to dryness. The beakers were allowed to cool down and then covered with cling films.

Step 4: Before running samples on the ICP-MS, small holes in the cling films were made, and 5 ml of 10% HNO_3 were added through the holes. The beakers were put in a microwave, heated for 13 seconds on a power level 10, and allowed to cool down. Finally, the solutions were transferred to small washed tubes for ICP-MS analysis. The solutions for ICP-MS analysis were prepared and analyzed by Dr. Apichet Boonsoong.

Loss on ignition was carried out at the Department of Geological Sciences, Faculty of Science, Chiang Mai University by the author via a gravimetric method, i.e. heating about 1 g of each sample powder at 1000°C for 12 hours.

The analytical results for major oxides and trace elements of the studied volcanic samples and hypabyssal samples are reported in Table 4.1 and the REE analyses of representative samples are given in Table 4.2.

4.3 ELEMENT MOBILITY

Although the studied mafic volcanic rocks and hypabyssal rocks were carefully selected, their chemical compositions are unlikely to represent those in magma since the rocks have undergone variable degrees of alteration (see Chapter 3). The secondary processes may lead to the removal and addition of mobile elements. The concentrations of immobile elements may be changed, due to the dilution or enrichment of the mobile elements; however, the ratios of immobile elements in the

Table 4.1 Whole-rock analyses and some selected ratios of the studied least-altered volcanic rocks and hypabyssal rocks.

Sample no.	MT-2**	MT-4**	MT-5**	MP-1**	MP-4**	MP-6**
Major oxide (wt%)						
SiO_2	63.37	54.72	58.57	55.32	55.07	54.06
TiO_2	0.90	1.13	1.01	1.15	1.13	1.16
Al_2O_3	16.19	17.82	16.78	17.93	17.69	17.98
FeO*	4.47	6.90	6.02	6.37	6.79	6.74
MnO	0.07	0.13	0.11	0.14	0.14	0.14
MgO	1.26	3.61	2.70	3.51	3.56	3.45
CaO	3.06	7.60	5.90	7.88	7.83	7.35
Na_2O	3.35	2.97	2.63	3.15	2.68	2.76
K_2O	4.20	2.07	3.10	1.84	1.92	2.30
P_2O_5	0.34	0.41	0.37	0.43	0.42	0.43
LOI	1.60	2.19	1.91	2.30	2.44	2.46
Sum	98.81	99.55	99.10	100.02	99.68	98.83
FeO*/MgO	3.55	1.91	2.23	1.81	1.91	1.95
Trace elements (ppm)						
Rb	157	75	122	71	66	75
Sr	342	500	530	606	594	449
Y	30	26	36	25	27	25
Zr	229	153	234	181	183	141
Nb	10	5.9	8.7	5.9	5.5	6.3
Ni	14	29	11	29	27	29
Cr	18	63	9.4	73	56	59
V	120	179	156	182	187	186
Sc	8.9	26	13	19	24	25
Hf	6.5	5.4	4.7	4.6	3.4	3.7
Ta	1.2	1.6	1.1	1.1	< 1	< 1
Th	17	8.3	14	7.1	6.8	8.0
Selected element ratios						
Zr/TiO_2	0.025	0.013	0.022	0.015	0.016	0.012
Nb/Y	0.352	0.224	0.244	0.235	0.203	0.253
Nb/Zr	0.05	0.04	0.04	0.03	0.03	0.04
Y/Zr	0.13	0.17	0.15	0.14	0.15	0.18

FeO* = total iron as FeO; LOI = loss on ignition.
Oxides other than LOI, and trace elements were analyzed by XRF.
** = volcanic rock; *** = hypabyssal rock.

Table 4.1 Continued

Sample no.	MP-7**	MP-9**	MP-10**	MP-12**	MP-13**	MP-14**
Major oxide (wt%)						
SiO_2	54.58	59.90	59.81	55.46	55.76	54.57
TiO_2	1.14	0.99	1.00	1.17	1.13	1.13
Al_2O_3	17.79	16.40	16.43	17.80	17.73	17.47
FeO*	6.52	5.51	5.38	6.42	6.59	6.79
MnO	0.13	0.12	0.12	0.13	0.14	0.14
MgO	3.55	2.12	2.08	3.33	3.53	3.60
CaO	7.83	5.34	5.69	7.96	7.62	7.85
Na_2O	2.76	3.05	2.83	2.89	3.03	2.58
K_2O	2.04	3.02	3.04	1.90	2.12	1.87
P_2O_5	0.42	0.37	0.38	0.43	0.43	0.42
LOI	1.96	1.97	1.87	2.37	2.03	2.10
Sum	98.71	98.79	98.63	99.85	100.12	98.52
FeO*/MgO	1.84	2.60	2.59	1.93	1.87	1.89
Trace elements (ppm)						
Rb	67	110	111	69	71	76
Sr	459	488	494	590	480	565
Y	22	32	29	28	23	26
Zr	137	250	210	192	151	145
Nb	5.9	9.2	9.5	6.5	5.4	6.4
Ni	30	12	15	27	27	28
Cr	69	16	< 6	61	67	67
V	180	149	155	193	172	177
Sc	24	17	23	19	18	22
Hf	5.0	5.1	4.6	3.5	4.8	4.6
Ta	1.2	1.2	1.4	< 1	1.3	1.7
Th	7.0	11	12	7.1	7.2	8.7
Selected element ratios						
Zr/TiO_2	0.012	0.024	0.020	0.016	0.013	0.012
Nb/Y	0.268	0.284	0.326	0.233	0.234	0.250
Nb/Zr	0.04	0.04	0.05	0.03	0.04	0.04
Y/Zr	0.16	0.13	0.14	0.15	0.15	0.18

FeO* = total iron as FeO; LOI = loss on ignition; and Nd = not determined.
Oxides other than LOI, and trace elements were analyzed by XRF.
** = volcanic rock; *** = hypabyssal rock.

Table 4.1 Continued

Sample no.	MR-5**	MR-5.3**	MR-6**	MR-8**	MR-9***	MR-10**
Major oxide (wt%)						
SiO_2	48.19	56.33	52.60	51.33	49.36	59.12
TiO_2	1.12	0.94	0.95	0.80	1.08	0.84
Al_2O_3	19.18	18.93	17.29	16.14	18.31	17.94
FeO*	8.90	5.22	8.23	8.09	8.58	4.74
MnO	0.14	0.13	0.13	0.15	0.18	0.07
MgO	5.77	1.86	5.09	8.25	5.58	1.80
CaO	9.15	6.06	8.27	9.89	8.39	4.01
Na_2O	2.21	3.64	1.98	2.16	3.06	4.40
K_2O	1.97	2.05	2.79	1.00	1.67	3.41
P_2O_5	0.38	0.39	0.31	0.18	0.37	0.34
LOI	3.01	4.31	2.51	1.65	2.46	2.57
Sum	100.01	99.86	100.13	99.64	99.03	99.22
FeO*/MgO	1.54	2.81	1.62	0.98	1.54	2.64
Trace elements (ppm)						
Rb	53	96	68	45	58	129
Sr	647	943	449	387	744	524
Y	24	32	21	21	23	31
Zr	174	281	114	93	170	205
Nb	5.7	8.5	4.1	< 2	5.9	7.4
Ni	30	6.9	22	72	29	15
Cr	57	11	82	381	63	> 6
V	242	131	187	199	232	119
Sc	32	22	22	38	24	22
Hf	3.3	5.9	4.2	3.0	3.1	6.6
Ta	< 1	1.65	< 1	< 1	< 1	1.35
Th	4.9	10.3	7.1	5.3	5.6	14.5
Selected element ratios						
Zr/TiO_2	0.015	0.029	0.012	0.011	0.015	0.024
Nb/Y	0.244	0.261	0.191	< 0.094	0.261	0.236
Nb/Zr	0.03	0.03	0.04	< 0.02	0.03	0.04
Y/Zr	0.14	0.12	0.19	0.23	0.13	0.15

FeO* = total iron as FeO; LOI = loss on ignition.
Oxides other than LOI, and trace elements were analyzed by XRF.
** = volcanic rock; *** = hypabyssal rock.

Table 4.1 Continued

Sample no.	MR-10.3**	MR-11**	MR-12**	PM-1**	PM-4**	PM-5**
Major oxide (wt%)						
SiO_2	60.31	51.73	51.74	59.90	55.69	55.53
TiO_2	0.84	0.94	1.01	0.72	1.13	1.08
Al_2O_3	17.95	16.84	17.65	16.17	17.07	16.75
FeO*	4.17	8.79	8.25	4.95	7.11	7.49
MnO	0.10	0.20	0.17	0.54	0.14	0.16
MgO	1.56	5.89	4.77	3.65	3.84	3.92
CaO	5.36	8.21	8.54	2.25	5.41	5.98
Na_2O	3.71	2.08	2.75	4.96	3.99	3.19
K_2O	2.26	2.25	2.15	2.85	1.15	2.41
P_2O_5	0.36	0.23	0.34	0.18	0.35	0.35
LOI	2.34	2.25	2.55	3.25	3.26	2.33
Sum	98.97	99.40	99.92	99.42	99.14	99.19
FeO*/MgO	2.67	1.49	1.73	1.36	1.85	1.91
Trace elements (ppm)						
Rb	95	60	53	122	80	98
Sr	940	345	679	698	848	665
Y	31	18	21	22	30	27
Zr	262	79	173	164	190	150
Nb	7.3	4.0	6.8	6.2	6.3	6.5
Ni	14	36	27	23	13	13
Cr	< 6	149	60	50	24	34
V	122	209	198	133	247	221
Sc	7.3	28	29	13	26	21
Hf	6.4	4.1	3.1	6.2	4.2	4.3
Ta	1.1	< 1	< 1	< 1	1.1	< 1
Th	10.4	6.2	4.6	12.9	9.3	11.3
Selected element ratios						
Zr/TiO_2	0.030	0.008	0.017	0.022	0.016	0.013
Nb/Y	0.232	0.218	0.329	0.280	0.210	0.238
Nb/Zr	0.03	0.05	0.04	0.04	0.03	0.04
Y/Zr	0.12	0.23	0.12	0.14	0.16	0.18

FeO* = total iron as FeO; LOI = loss on ignition.
Oxides other than LOI, and trace elements were analyzed by XRF.
** = volcanic rock; *** = hypabyssal rock.

Table 4.1 Continued

Sample no.	BK-2***	BK-3**	BK-5**
Major oxide (wt%)			
SiO_2	48.12	51.94	48.96
TiO_2	1.13	1.40	1.65
Al_2O_3	17.57	17.05	18.88
FeO*	7.53	8.50	9.00
MnO	0.21	0.23	0.15
MgO	5.93	4.06	6.73
CaO	9.23	3.74	3.51
Na_2O	3.32	6.14	3.73
K_2O	1.53	1.55	1.75
P_2O_5	0.20	0.35	0.40
LOI	3.72	3.17	4.38
Sum	98.48	98.14	99.14
FeO*/MgO	1.27	2.09	1.34
Trace elements (ppm)			
Rb	68	82	88
Sr	694	356	384
Y	22	32	39
Zr	97	191	201
Nb	<2	5.1	7.5
Ni	68	25	88
Cr	150	65	13
V	235	247	354
Sc	36	29	43
Hf	4.6	4.9	4.9
Ta	< 1	2.0	< 1
Th	7.4	22	12
Selected element ratios			
Zr/TiO_2	0.0081	0.013	0.012
Nb/Y	< 0.091	0.157	0.193
Nb/Zr	< 0.02	0.03	0.04
Y/Zr	0.23	0.17	0.19

FeO* = total iron as FeO; LOI = loss on ignition.
Oxides other than LOI, and trace elements were analyzed by XRF.
** = volcanic rock; *** = hypabyssal rock.

Table 4.2 REE analyses (ppm) and some selected chondrite-normalized ratios of the studied least-altered volcanic rocks.

Sample no.	MT-4	MT-5	MR-10	PM-1	BK-3
La	32.4	43.8	41.6	30.6	37.3
Ce	66.3	89.4	84.2	56.2	74.2
Pr	6.90	9.3	8.9	5.8	7.8
Nd	33.10	43.2	39.3	25.2	36.5
Sm	6.68	8.56	7.84	4.92	7.33
Eu	1.72	1.89	1.80	1.28	1.77
Gd	5.34	6.61	5.84	4.12	6.02
Dy	4.59	5.71	5.20	3.81	5.54
Ho	0.97	1.19	1.07	0.83	1.17
Er	2.60	3.30	3.00	2.23	3.14
Yb	2.30	2.81	2.68	2.03	2.64
Lu	0.38	0.49	0.46	0.36	0.44
Selected ratios					
[La/Sm]cn	2.96	3.12	3.23	3.10	3.79
[Sm/Yb]cn	3.15	3.30	3.17	2.63	3.01

primary rock and altered rock remain constant. Accordingly, only the elements considered as immobile elements, and immobile-element ratios are used in interpreting the geochemical data presented in this study.

Almost all the major oxides, excluding some certain minor oxides, in igneous rocks are sensitive to alteration/metamorphic processes. It is, however, generally agreed that the values of total iron and MgO in the carefully selected samples of altered/metamorphosed igneous suites are little removed from primary values. According to the little mobility of total iron and MgO, and their significant abundances in mafic volcanic rocks, total iron as FeO (herein FeO*)/ MgO ratios are used as a fractionation parameter for the studied least-altered volcanic samples.

Following the work pioneered by Pearce and Cann (1971, 1973), numerous studies have shown that the high field strength elements (herein HFSE) Ti, Zr, Y, Nb,

Ta, Th, U and P, and also the transitional elements Ni, Cr, V and Sc are relatively immobile during the alteration of basaltic and more evolved lavas and intrusives. In addition, although occasional reports have appeared of REE-, especially light REE (herein LREE), mobility during hydrothermal alteration and low-grade metamorphism (e.g. Hellman and Henderson, 1979; Whitford *et al.*, 1988), the overwhelming consensus of opinion is that the REE patterns of carefully selected igneous samples are probably slightly shifted from their primary patterns, but remain parallel/sub-parallel to the primary patterns. Consequently, in attempting to determine the geochemical affinities and tectonic significance of the studied least-altered mafic volcanic rocks and hypabyssal rocks, concentration has focused on the relatively immobile elements, namely HFSE, REE and transition elements.

4.4 MAGMATIC AFFINITY

The studied least-altered volcanic rocks span the ranges in Zr/TiO_2 and Nb/Y from 0.008 to 0.030 and <0.094 to 0.352, respectively, whereas the presented hypabyssal rocks have the values for Zr/TiO_2 = 0.008 and 0.015, and and Nb/Y = <0.091 and 0.261 (Table 4.1). Accordingly, the volcanic rocks are classified as subalkalic andesite (sample numbers MT-2, MT-5, MP-1, MP-4, MP-9, MP-10, MP-12, MR-5, MR-5.3, MR-8, MR-10, MR-10.3, MR-12, PM-1 and PM-4) and andesite/basalt (sample numbers BK-3, BK-5, MP-6, MP-7, MP-13, MP-14, MR-6, MR-11, MT-4 and PM-5) based on the nomenclature given by Winchester and Floyd (1977) as illustrated in Figure 4.1. Similarly, the hypabyssal rocks are microdiorite (sample number MR-9) and microdiorite/microgabbro (sample number BK-2), which are the plutonic equivalents of the andesite and andesite/basalt in respect manner.

The FeO*/MgO variation diagrams for immobile major oxides (Fig. 4.2) and trace elements (Fig. 4.3) show that both the studied volcanic samples and hypabyssal samples have similar chemical compositions, suggesting either a common source rock or a common parental magma. Although the rocks are undoubtedly subalkalic, their calc-alkalic or tholeiitic nature cannot be positively specified, due to the rather

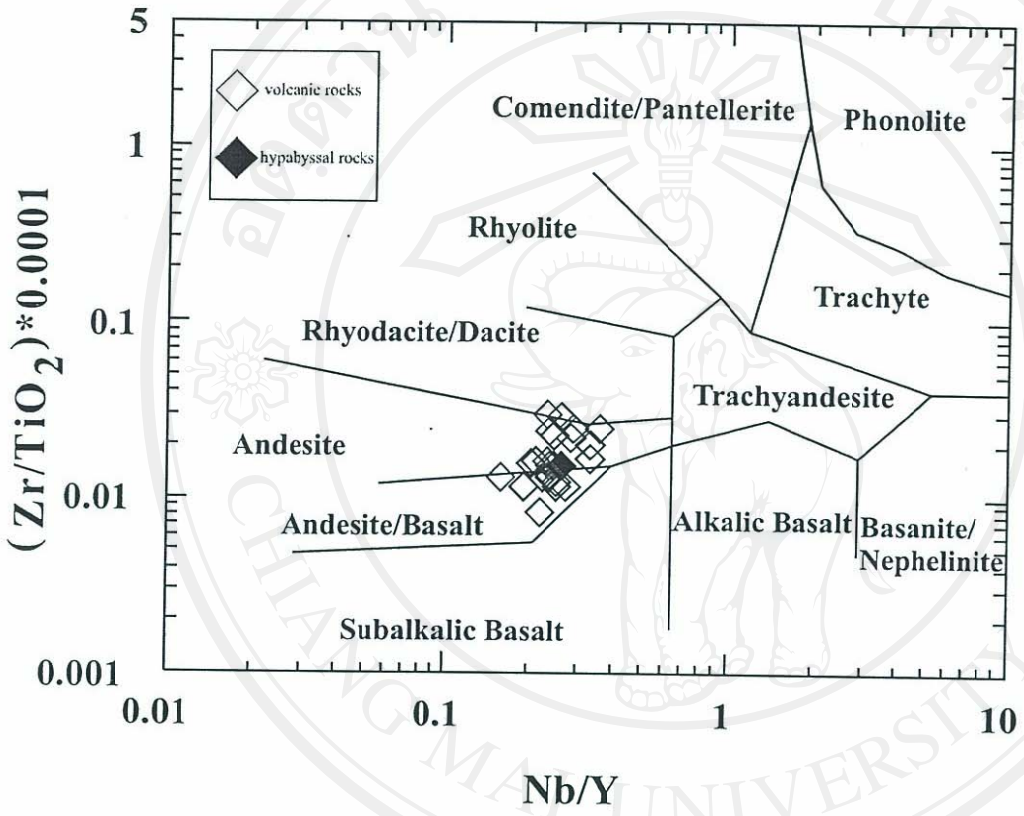

Figure 4.1 Plot of Zr/TiO_2 against Nb/Y for the studied least-altered volcanic rocks (open diamond) and hypabyssal rocks (solid diamond). Field boundaries for different magma types are taken from Winchester and Floyd (1977). The data points for rocks with Nb content below the detection limit are omitted.

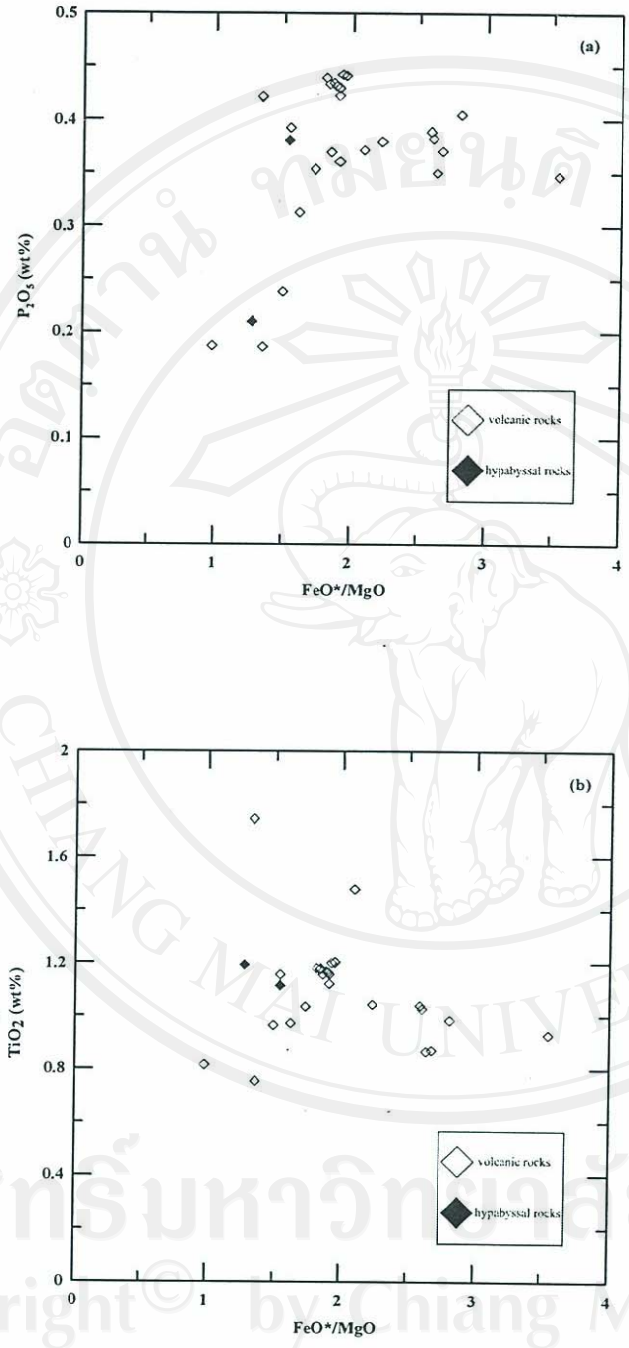

Figure 4.2 FeO*/MgO variation diagrams for (a) P_2O_5 and (b) TiO_2 of the studied least-altered volcanic rocks (open diamond) and hypabyssal rocks (solid diamond).

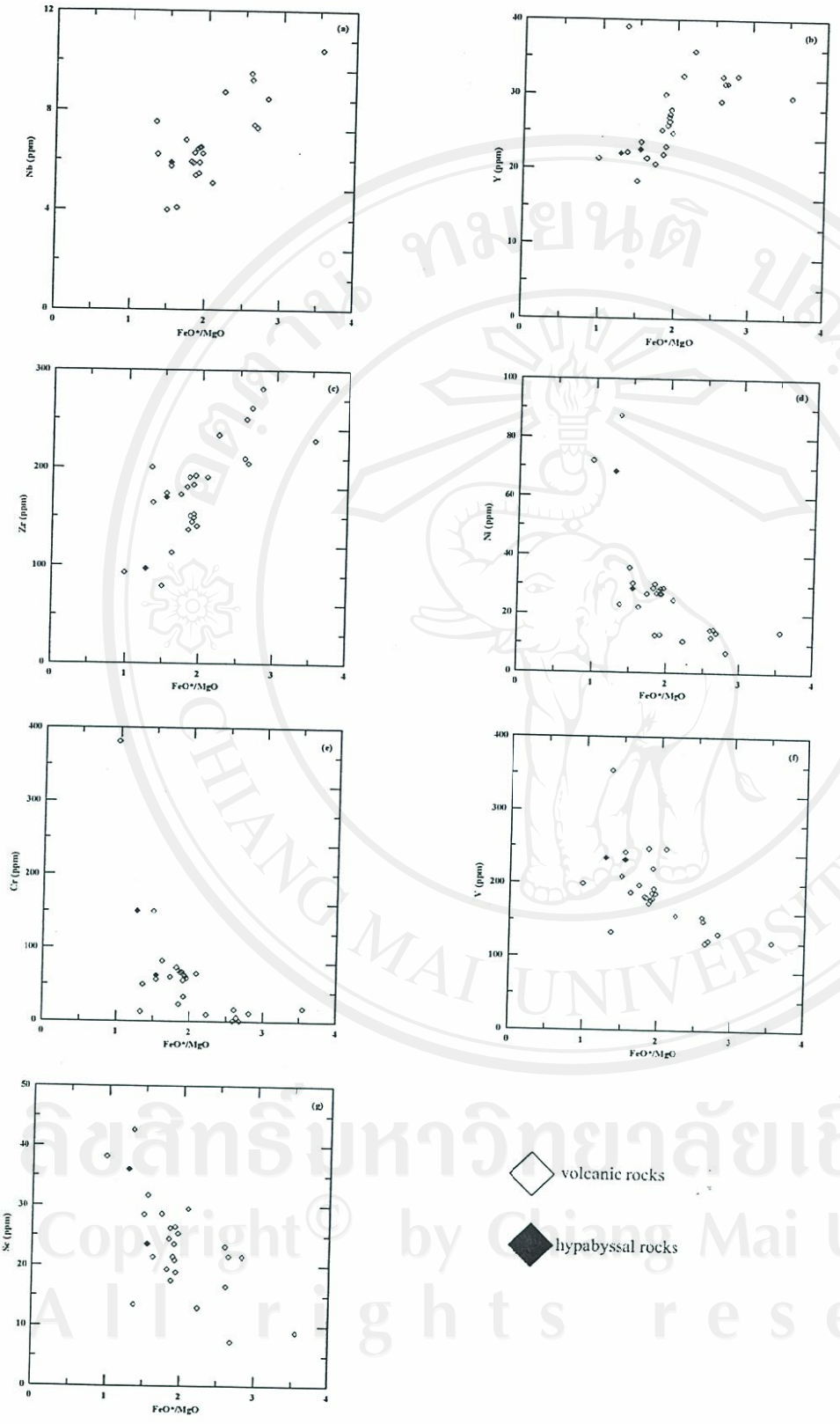

Figure 4.3 FeO*/MgO variation diagrams for (a) Nb, (b) Y, (c) Zr, (d) Ni, (e) Cr, (f) V and (g) Sc for the studied least-altered volcanic rocks (open diamond) and hypabyssal rocks (solid diamond). The data points for rocks with Nb content below the detection limit are omitted from (a).

constant chemical patterns for TiO_2 and V. P_2O_5, Nb, Zr and Y form broadly positive trends against FeO*/MgO, typical of incompatible element behavior, while the trends Ni, Cr and Sc descend relative to FeO*/MgO, recording possible olivine, pyroxene and chrome-spinel removal. The pyroxene fractionation is in agreement with the occurrences of clinopyroxene and orthopyroxene (completely altered) phenocrysts/microphenocrysts as previously discussed in Chapter 3.

The relationships between incompatible-element pairs for the studied volcanic rocks and hypabyssal rocks, such as Nb-Zr and Y-Zr (Fig. 4.4) reveal that the data points for the studied samples form positive trends that cannot be traced back to zero. These imply that the studied samples have not been formed by eutectic melting of a common source rock with different degrees of partial melting, but have formed by different degrees of crystal fractionation from a common parental magma, with different bulk distribution coefficients for mineral removals. Ti appears to be constant, when Zr is used as a fractionation parameter (Fig. 4.4), typical of calc-alkalic affinity (Pearce and Cann, 1973).

The REE patterns of five representative samples (Fig. 4.5) show LREE enrichment and relatively flat heavy REE (herein REE), with chondrite-normalized values for La/Sm [herein (La/Sm)cn] and Sm/Yb [herein (Sm/Yb)cn] ranging from 2.96 to 3.79 and 2.63 to 3.30, respectively. These are characteristic features of mafic calc-alkalic lavas (e.g. Wilson 1990), corresponding to the deduction from the pattern on Ti – Zr plot (Fig. 4.4). The calc-alkalic nature is also well supported by the positions of the studied samples on ternary diagrams Ti–Zr–Y (Fig. 4.6), Hf–Th–Ta (Fig. 4.7) and Y–La–Nb (Fig. 4.8), although the applied diagrams were designed for basalts.

4.5 TECTONIC SETTING OF ERUPTION

Many tectonic discrimination diagrams have been applied to the studied least-altered volcanic samples and hypabyssal samples. The studied volcanic rocks appear to

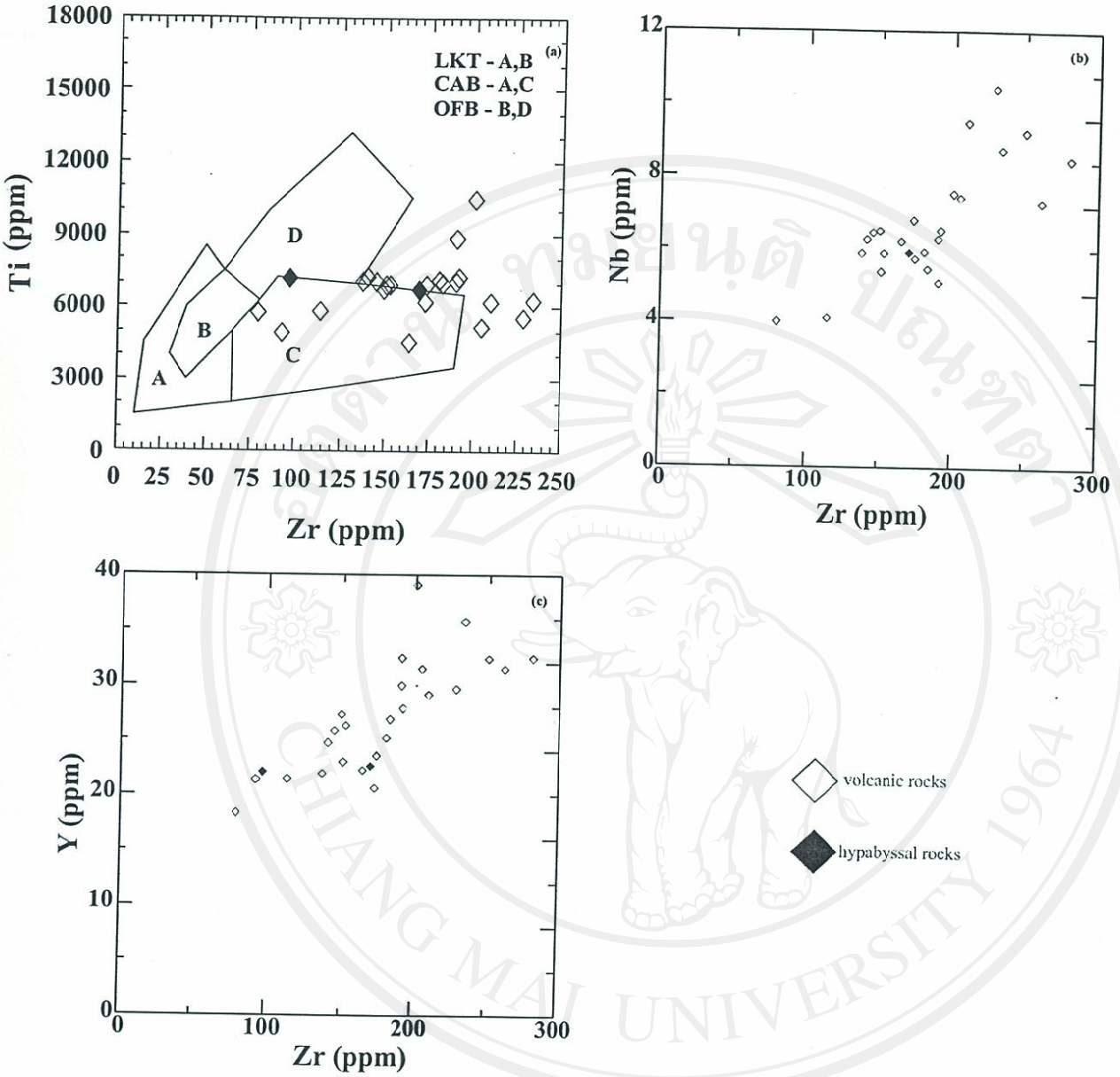

Figure 4.4 Plots of (a) Ti, (b) Nb and (c) Y against Zr for the studied least-altered volcanic rocks (open diamond) and hypabyssal rocks (solid diamond). The data points for rocks with Nb content below the detection limit are omitted from (b). The boundaries beween different tectonic settings (LKT = low-K tholeiite, CAB = calc-alkalic basalt, and MORB = mid-ocean ridge basalt) are after Pearce and Cann (1973).

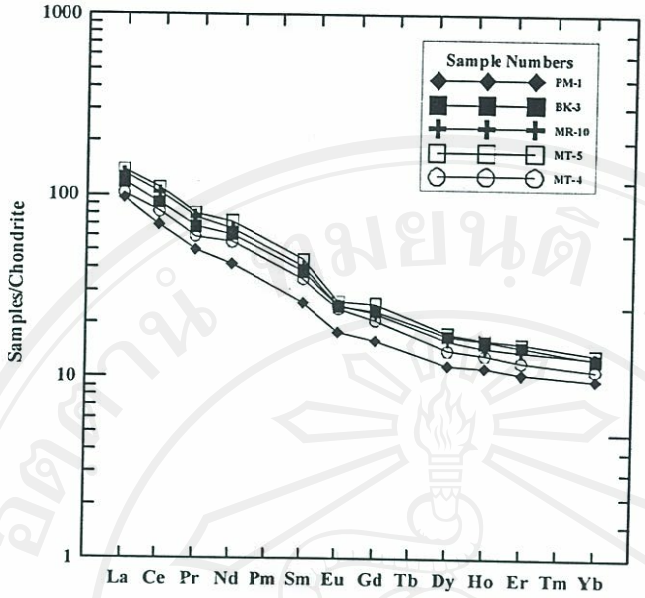

Figure 4.5 Chondrite-normalized REE patterns for the representative, least-altered, volcanic rocks presented in this study. The normalizing values used are those of Taylor and Gorton (1977).

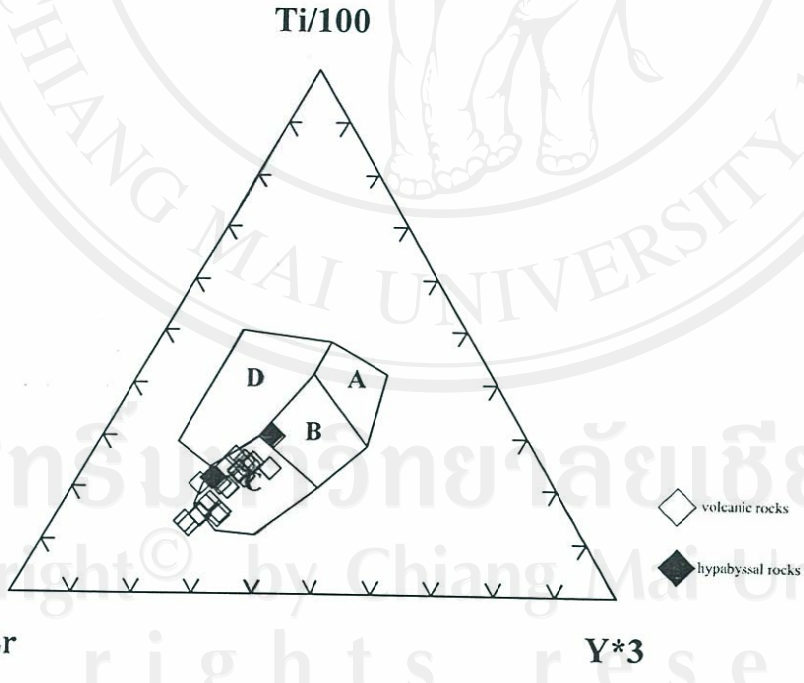

Figure 4.6 Ti- Zr-Y tectonic discrimination diagram (after Pearce and Cann, 1973) for the studied least-altered volcanic rocks (open diamond) and hypabyssal rocks (solid diamond). A = island-arc tholeiites, B = MORB, island-arc tholeiites and calc-alkalic basalts, C = calc-alkalic basalts and D = within-plate basalts.

be plate-margin basalt (erupted along an active continental margin, an oceanic island arc and a mid-oceanic ridge) on a Ti/Y against Zr/Y diagram (Fig. 4.9). The volcanic-arc environment is supported by their positions on the plots of Ti-Zr (Fig. 4.4), Ti-Zr-Y (Fig. 4.6), Hf-Th-Ta (Fig. 4.7), La-Nb-Y (Fig. 4.8), and Nb-Zr-Y (Fig. 4.10). The studied mafic rocks, however, appear to be back-arc basin basalt on a Ti-V plot (Fig. 4.11) and within-plate basalt on a Zr/Y-Zr diagram (Fig. 4.12).

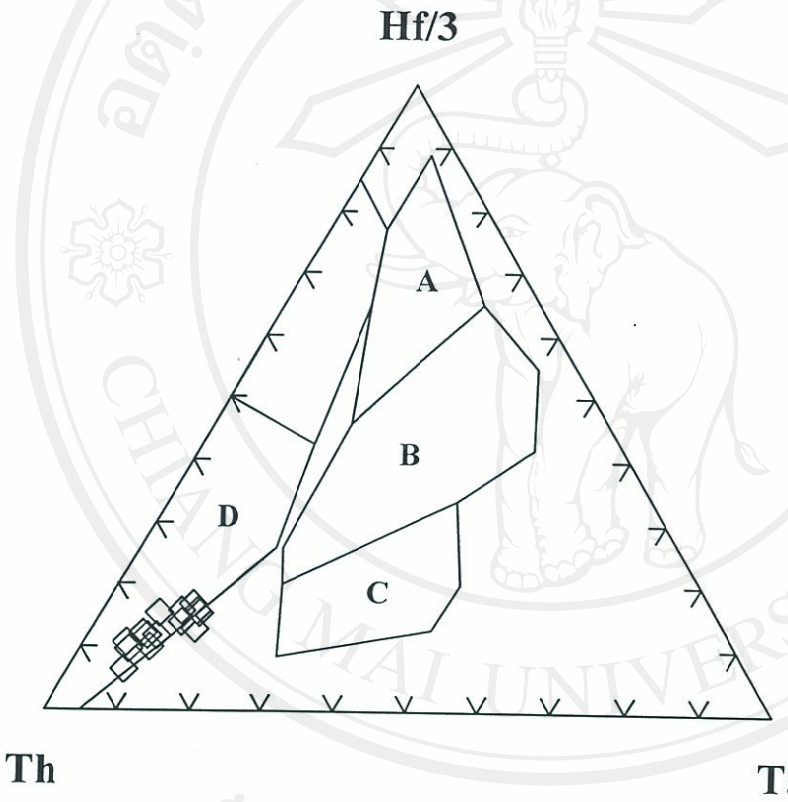

Figure 4.7 Ternary Hf-Th-Ta tectonic discrimination diagram (after Wood, 1980) for the studied least-altered volcanic rocks. The broken line shows an Hf/Th ratio of 3. A = N-type MORB, B = E-type MORB and within-plate tholeiites, C = within-plate alkalic basalts, and D = calc-alkalic basalts (Hf/Th<3) and island-arc tholeiites (Hf/Th>3). The data points for rocks with Ta content below the detection limit are omitted.

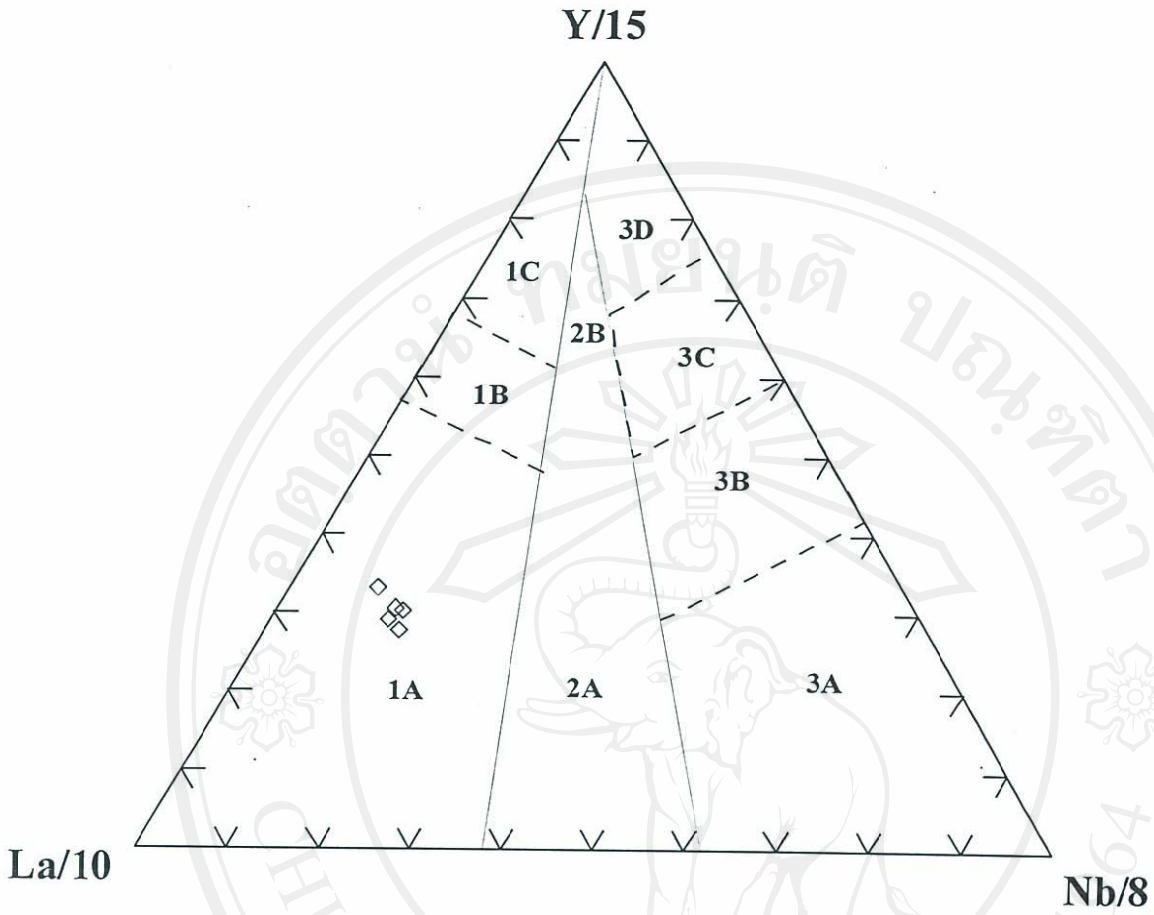

Figure 4.8 La-Y-Nb tectonic discrimination diagram (after Cabanis and Lecolle, 1989) for the representatives of the studied least-altered volcanic rocks. Field 1 contains volcanic-arc basalts, field 2 continental basalts and field 3 oceanic basalts. The subdivisions of the fields are as follows: 1A = calc-alkalic basalts, 1C = volcanic-arc tholeiites, 1B is an overlap between 1A and 1C, 2A = continental basalts, 2B = back-arc basin basalts, 3A = alkalic basalts from intercontinental rift, 3B and 3C = E-type MORB (3B enriched and 3C weakly enriched), and 3D = N-type MORB.

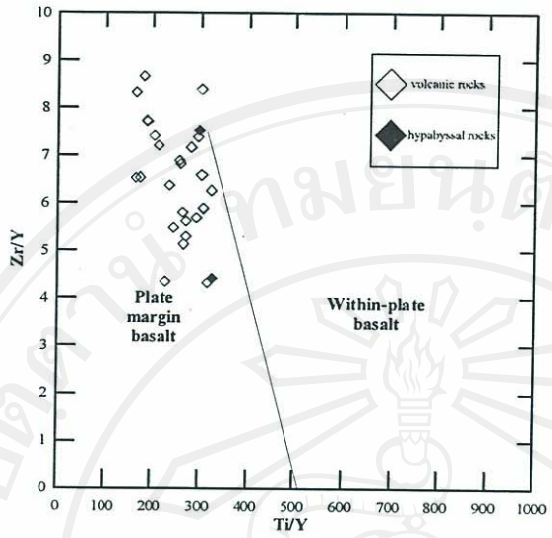

Figure 4.9 Zr/Y-Ti/Y tectonic discrimination diagram (after Pearce and Gale, 1977) for the studied least-altered volcanic rocks (open diamond) and hypabyssal rocks (solid diamond).

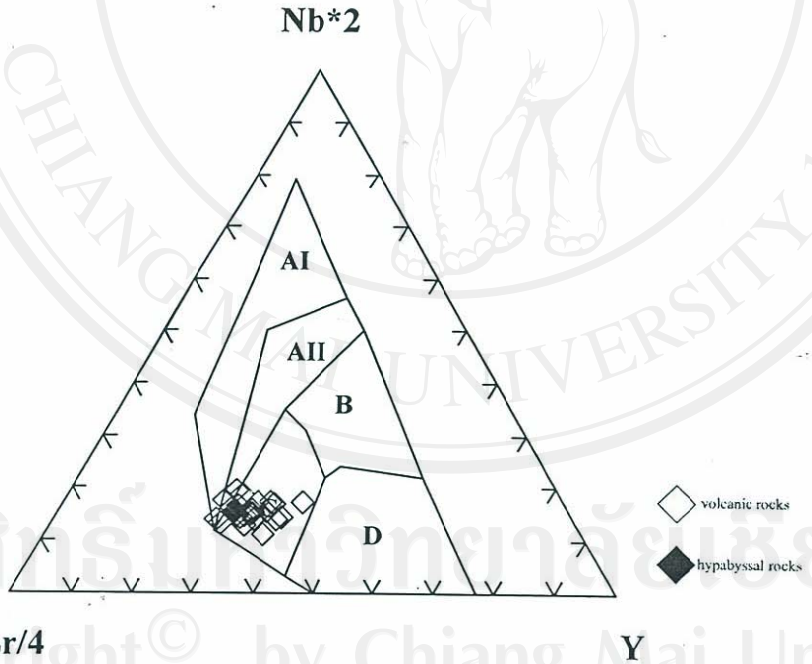

Figure 4.10 Zr-Nb-Y tectonic discrimination diagram (after Meschede, 1986) for the studied least-altered volcanic rocks (open diamond) and hypabyssal rocks (solid diamond). AI = within-plate alkalic basalts, AII = within-plate alkalic basalts and within-plate tholeiites, B = E-type MORB, C = within-plate tholeiites and volcanic-arc basalts, and D = N-type MORB and volcanic arc basalts. The data points for rocks with Nb content below the detection limit are omitted.

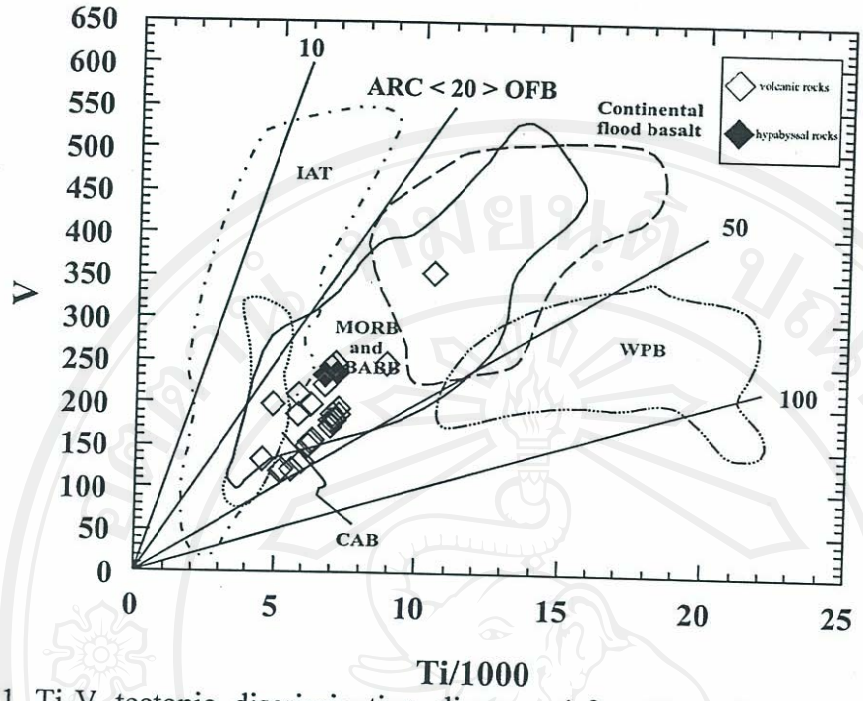

Figure 4.11 Ti-V tectonic discrimination diagram (after Shervais, 1982) for the studied least-altered volcanic rocks (open diamond) and hypabyssal rocks (solid diamond). The numbers given along the solid straight lines are Ti/V ratios. IAT = island-arc tholeiites, BABB = back-arc basin basalts, WPB = within-plate basalts, and CAB = calc-alkalic basalts.

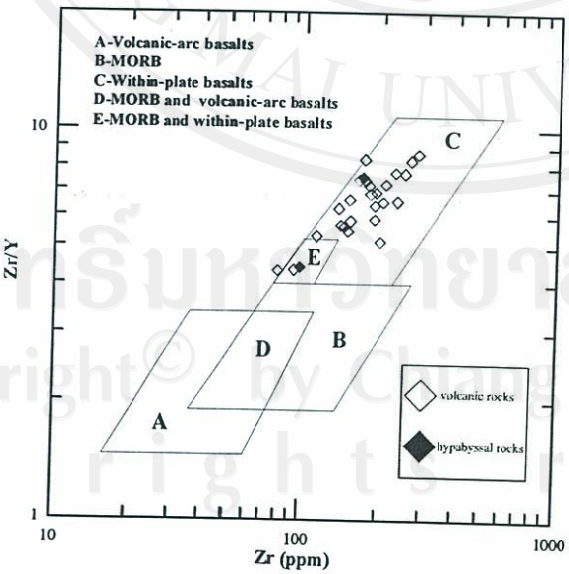

Figure 4.12 Zr/Y – Zr discrimination diagram (after Pearce and Norry, 1979) for the studied least-altered volcanic rocks (open diamond) and hypabyssal rocks (solid diamond).

Up to now, many tectonic discrimination diagrams for either mafic or felsic volcanic rocks have been constructed. However, several studies (Holm, 1982; Prestvik, 1982; Duncan, 1987; and Myers and Breitkopf, 1989) have demonstrated that these diagrams may often fail to unequivocally classify tectonic setting of formation of altered lavas. In order to solve the problem, the classical principle of geology "Present is the key to the past" has been applied. In the other words, if the tectonic interpretation is correct, there should be modern analogs (Panjasawatwong, 1991, 1999; Panjasawatwong *et al.*, 1995, 2003, 2006; Phajuy *et al.*, 2005; Singharajwarapan *et al.*, 2000; Barr *et al.*, 2000). Extensive searches for modern analogs have been made in terms of chondrite and N-MORB normalized multi-element patterns. In doing so, the representatives of the andesite/basalt samples presented in this study are analogous to the calc-alkalic basalt and basaltic andesite from Salina, Aeolian Arc, Italy (Gertisser and Keller, 2000) that erupted in an active continental margin, which is linked to the complex collision between the Africa and European plates in the Mediterranean (Fig. 4.13). Consequently, the studied andesite/basalt and microdiorite/microgabbro are interpreted to have erupted in an active continental margin that is linked to the complex collision between Shan-Thai and Indochina cratons.

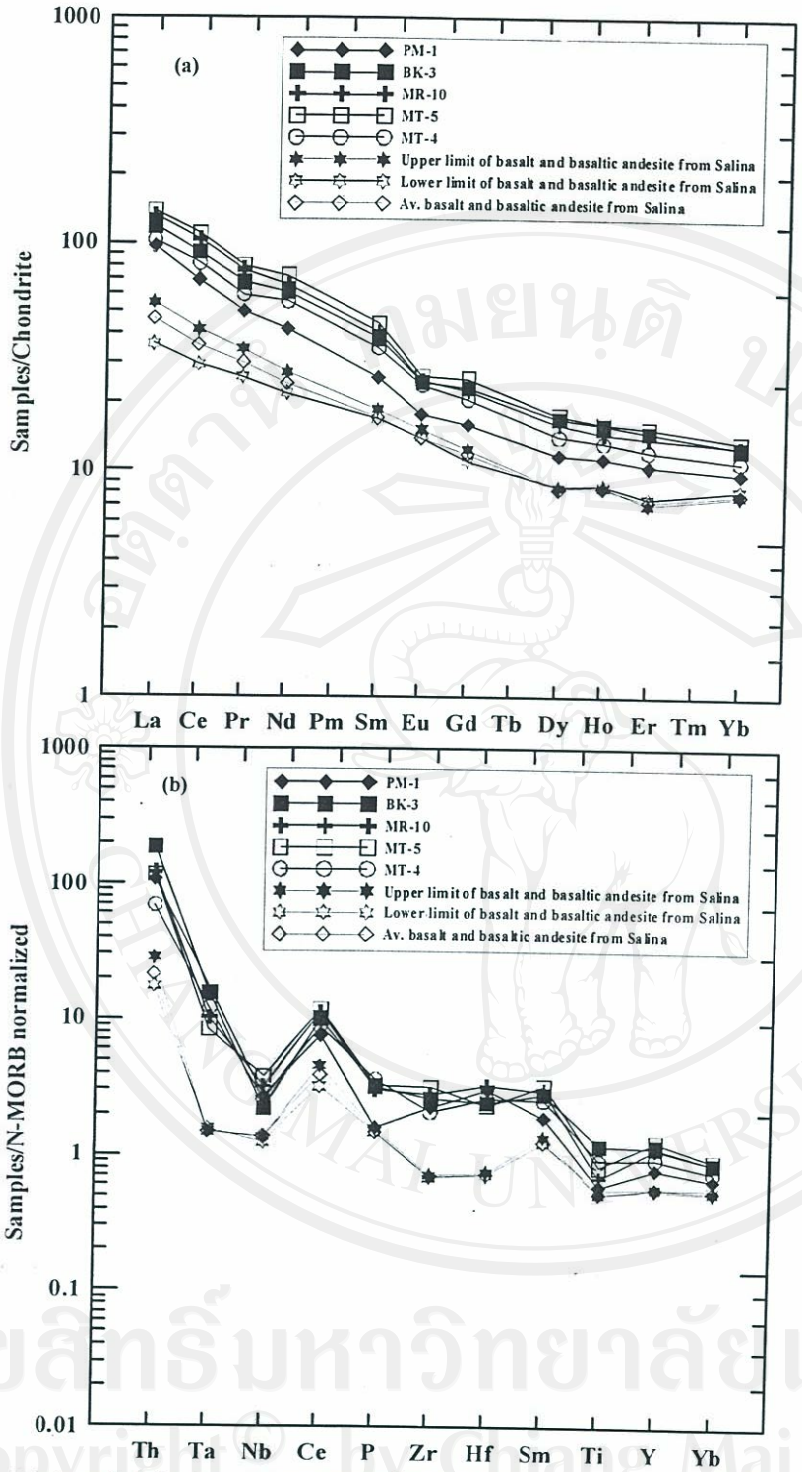

Figure 4.13 Plots of (a) chondrite-normalized REE and (b) N-MORB normalized multi-elements for the representative volcanic rocks presented in this study, and their modern analogs, calc-alkalic basalt and basaltic andesite from Salina Island, Aeolian Arc, Italy (Gertisser and Keller, 2000). Chondrite-normalizing values are those of Taylor and Gorton (1977), whereas N-MORB normalizing values are those of Sun and Mcdonough (1989).